Journal of the Oceanographical Society of Japan
Vol. 35, pp. 151 to 167, 1979

Prediction of Ocean Waves Based on the Single-Parameter Growth Equation of Wind Waves*

Sanshiro KAWAI**, Paimpillil S. JOSEPH** and Yoshiaki TOBA**

Abstract: A method for the prediction of ocean waves was developed on the basis of the single-parameter growth equation of wind waves, proposed by TOBA (1978) on the basis of similarity in growing wind waves. The applicability of the method to actual problems was tested by hindcasting the wave characteristics with the method, for two cases with differing time and space scales, one in Kii Channel Approach, Japan, and the other in the North Atlantic Ocean. The results showed that the present method can predict waves within an error of 1.3 m in wave heights, which ranged from 3 to 12 m.

1. Introduction: Physical background of the present prediction method

Methods of ocean wave prediction in practical use may be classified into two classes, that is, a representative- (or significant-) wave method and a spectrum method. This classification is based on differences in the statistical representation of oceanic wave field. In the former method, it is expressed by a set of height and period of representative waves, whose special case is the significant waves. In the latter, it is expressed by the superposition of many frequency and directional component waves with differing heights. The relative advantages of the two classes will be discussed later.

Whichever class we choose, we have to rely on empirical relations to some extent, since our knowledge of the growth mechanism of wind waves is very limited. The combined mechanism of PHILLIPS (1957) and MILES (1957) had been considered to be the final solution of the growth mechanism of wind waves for about ten years following their proposition, but later it was seen to be ineffective with the accumulation of experimental data. BARNETT and KENYON (1975) in a review paper concluded that since then "no new complete theory has yet appeared, although a few new suggestions have been put forward." As an example of the new suggestions, besides those reviewed by them, we can point out the explanation of the growth processes of individual wave crests given by OKUDA (MS: see References) which was proposed on the basis of detailed observation of flow in the water relative to the individual crests of wind waves. Since the mechanisms by PHILLIPS and MILES are ineffective in giving actual growth rate of wind waves, and the linear and exponential timewise growth rates of wind waves used in the prediction models based on the spectrum concept are empirical ones, it is unreasonable to call them "Phillips' and Miles' growth rates", respectively. In this connection, it is noteworthy that KAWAI (1979) showed that the initiation of wind waves can be explained by a linear instability mechanism which is a slight modification of Miles' mechanism (1962), and also that the efficacy of the linear mechanism is limited to about 10 seconds from the onset of wind above a still water surface.

Although our knowledge about the growth mechanism is so limited, it has been recognized that there is a very simple similarity in growing wind waves, presumably due to the strong nonlinearity inherent in wind waves under the action of the wind, and this similarity contributes to the reduction of complexity in prediction models. The most conspicuous manifestation of the similarity is the three-seconds power law

$$H^* = BT^{*3/2} \qquad (1)$$

between the nondimensional wave height $H^* = gH/u_*^2$ and the non-dimensional period T^*

* Received May 1, revised Sept. 7 and accepted Oct. 11, 1979.

** Geophysical Institute, Faculty of Science, Tohoku University, Sendai 980, Japan

$=gT/u_*$ of the representative waves, first proposed by TOBA (1972) and later confirmed by KAWAI *et al.* (1977) and TOBA (1978), where u_* represents the friction velocity of air, g the acceleration due to gravity and B is a nondimensional constant equal to 0.062 for the case of significant waves. The similarity originates from the similarity structure of individual waves in wind waves as shown by TOKUDA and TOBA (MS: see References). This power law makes it possible to represent the state of the wind-wave field in terms of a single variable, for example, the representative wave height H, the period T, or the wave energy E per uint area of the sea surface. If we adopt the significant waves as the representative waves, there is a relation between H and E,

$$E=H^2/16\,, \qquad (2)$$

which was given by LONGUET-HIGGINS (1952). This type of relation can also be interpreted as a manifestation of the similarity of wind waves. Based on these considerations, TOBA (1978) proposed the following single-parameter growth equation of wind waves

$$\frac{\partial(E^{*2/3})}{\partial t^*}+\frac{E^{*1/3}}{a}\frac{\partial(E^{*2/3})}{\partial F^*} =G_0R[1-\mathrm{erf}(bE^{*1/3})] \qquad (3)$$

where $E^*=g^2E/u_*^4$, $F^*=gF/u_*^2$, F is the fetch, t the duration, erf the error function defined by

$$\mathrm{erf}(x)=\frac{2}{\pi^{1/2}}\int_0^x \exp(-\zeta^2)d\zeta\,, \qquad (4)$$

and the other variables are nondimensional empirical constants with the following values

$$G_0R=2.4\times10^{-4},\ a=0.74 \text{ and } b=0.12. \qquad (5)$$

Equation (3) states that the growth of nondimensional energy of wind waves is a simple stochastic process in which the single parameter representing it approaches to its final value, independent of its past history, but depending on its present state, so long as the wind continues to blow.

In this article, we intend to develop a method for the prediction of ocean waves based on the above single-parameter growth equation. In order to apply the equation to real situations, a few problems have to be overcome. The most serious problem is that the equation cannot be applied to swells in its original form, since it was introduced for the case of growing wind waves. In the next section, some empirical relations and appropriate assumptions by which these problems are overcome will be discussed.

As can be recognized from above, the present method belongs to the class of the representative wave method according to the classification at the beginning of the present article. To discuss the relative advantages of the two classes of the methods, it is necessary to discuss the cases of wind waves and swells separately. Since there is a similarity in the growing wind-wave field, the spectrum of wind waves has a similar form and it has mutually-transformable relationships with the quantities of representative waves, as discussed by TOBA (1978). Therefore, if the quantities of representative waves are predicted, the spectral quantities can also be estimated from these quantities through these relationships. On the other hand, if the prediction is performed with the spectrum method, the predicted spectrum might not satisfy the similarity relation due to some inadequacy of the model for prediction. Moreover, even if the predicted spectrum does satisfy the similarity relation, the prediction method wastes computational time. Thus, the representative wave method is considered better and more reasonable than the spectral method, for wind waves.

A somewhat similar method for wave prediction is the "parametric wave prediction model" developed by HASSELMANN *et al.* (1976). Their method predicts the scale parameters representing their similar spectral forms decided empirically. Since these para meters have definite relations with the properties of representative waves, their method resembles ours. Although the functional expressions of the similar spectral forms are different between theirs and Toba's (1978) 4th-power form, MITSUYASU *et al.* (MS: see References) showed that the actual difference of the spectral forms is small. In contrast with this apparent resemblance, their concept of the physical background seems much different from ours. They consider that the weakly nonlinear interactions between component waves work efficiently to adjust the spectral form to the similar one.

However, the computation to demonstrate the tendency of self-adjustment shown in HASSELMANN *et al.* (1973) was too limited, and did not include the effect of atmospheric input. From our point of view, the similarity in the growing wind-wave field originates from the strong coupling of wind and waves, including organized local wind drift and turbulence in wind waves (e.g. TOBA *et al.*, 1975; OKUDA, MS: see References).

In the case of swells, the method based on representative waves loses its applicability, because when swells predominate there is no similarity. For swells, the sea state uncouples with the wind, and the component waves are free from strong interaction with wind action and can propagate freely as simple water waves. In this case, the spectral method which is based on the component-wave concept, s better.

Thus, the two classes of methods have advantages and disadvantages relative to each other, and the disadvantages have to be covered by some empirical methods, when applied to the real sea state where wind waves and swells coexist.

To clarify the position of the proposed method among the many methods of prediction, we will review those which belong to the representative wave method. In the representative wave method, the wave prediction is based on the fetch graph originated by SVERDRUP and MUNK (1947) which has been revised several times in accordance with the accumulation of observational data. The term "fetch graph" expresses the empirical functional relations of the nondimensional wave height and period (or the corresponding quantities) to the nondimensional fetch, and the term "fetch" represents the distance over which wind blows, developing the wind waves. Hence, it is essentially a one-dimensional space coordinate. As a result, the concept "fetch" is difficult to fit into the real wind and wind-wave field, which is essentially two-dimensional. Various efforts to improve the representative wave method concentrated on overcoming this difficulty, in addition to improving of the fetch graph itself. We will discuss this point further in the next section, and show how the difficulty can be overcome in the present method.

The merits of the present method lie in the following points. In contrast to traditional method of parallel estimation of the wave height and period using two independent fetch graphs, the estimation of only one parameter E^* in (3) is sufficient for the prediction of wind-wave field in the present method. The wave height and period can be calculated from the value E^* with the relations (1) and (2) which are based on the similarity in wind waves. Consequently, the present method is better than the traditional ones which might predict a set of wave height and period which does not satisfy the similarity relation (1). Moreover, the computation itself is simpler.

Further, in physical interpretation, emphasis should be given to the fact that equation (3) is given by a simple stochastic form including an error function, in expressing the development of wind waves. However, the present method is similar to the methods of WILSON (1961) and IJIMA *et al.* (1967) in that the differential form of fetch graph is used, since the form of equation (3) was derived by TOBA (1978) from a functional approximation of the differential form of Wilson's (1965) fetch graph.

2. Numerical method of prediction

In this section, we will describe shortly the essential points of the numerical method for the prediction of ocean waves using the single-parameter growth equation. The detailed numerical scheme is shown in Appendix.

2-1. Wave-packet following method

We transform (3) into its total-derivative form as

$$\frac{d(E^{*2/3})}{dt^*} = G_0 R[1-\mathrm{erf}(bE^{*1/3})], \quad (6)$$

which represents, in a nondimensional form, the temporal growth rate of wave energy when an observer follows the wave packet. Since (6) is easier to treat than (3), we will predict the growth of ocean waves with this equation. The method based on (6) is hereafter called the "wave-packet following method." Equation (6) is a first order ordinary differential equation and can be easily integrated numerically. In the present study, (6) is integrated with an iteration method, shown in Appendix, which makes the relative error of the computation nearly uniform

throughout the paths of the wave packets. The number of iterations depends on the values of E and u_*. When $E=0$ and u_* is very small, the number may exceed 40. However, when E exceeds a small value, the number reduces remarkably, and the average number throughout a path of wave packets is about two. Because of this, when the present wave energy is zero, the fetch graph by WILSON (1965) is used directly for prediction of wave energy after Δt. In the numerical computation, it is assumed that the wind is constant in the interval Δt. Therefore, the fetch graph can be used in its original form, when the present energy is zero.

When the wave energy E is predicted, the wave height H can be calculated by the relation (2). The wave period T can be calculated by the three-seconds power law (1), from the wave height. With these procedures, we can predict the characteristics of the waves at the time Δt later, when the present value of their energy is given.

Next, we have to locate the position of the wave packet. This can be done by using the group velocity C_g of waves as follows. The distance ΔF of travel of the wave packet is calculated by

$$\Delta F = C_g \Delta t \qquad (7)$$

where C_g can be calculated from the wave period T, as

$$C_g = \frac{1}{2}\frac{g}{2\pi}T . \qquad (8)$$

The average value of T through the interval Δt is used in (8).

2-2. Wind direction and wave direction

For a uni-directional wind field, the computational procedures in *2-1* is enough to predict the wind waves developed in the wind field. However, since real wind fields vary spatially and temporally, we have to develop a method which is applicable to these fields. This is a problem common to the representative wave methods, as already mentioned. In general terms, we are encountering the problem of adapting the fetch graph, or similar relations, that is prepared in one-dimensional expressions, to the real two-dimensional field. In order to overcome the problem, two methods have been proposed so far. The first was Wilson's (1955), in which lines are drawn in the region considered, through the point where the waves have to be predicted, in advance of the prediction calculation, and each line is treated as one-dimensional coordinate of the fetch. Since the wind does not necessarily blow along these lines, some adequate measures of effective wind speed have to be made. He used the component of the wind along the lines as the wind speed for the prediction. In Wilson's method, the path line is arbitrarily decided in advance, therefore, the path line does not necessarily correspond to the real one. In the second method which was proposed by IJIMA *et al.* (1967), the path line of wave packets is assumed to coincide with the local wind direction, and the effect of the change of wave direction or the change of wind direction along the path line is evaluated separately. Since the wave direction is generally in near coincidence with the wind direction in the real state of the ocean, the second method is more natural, and we adopt it in the present study. In order to evaluate the effect of the change of wave direction $\Delta\theta$, IJIMA *et al.* (1967) proposed a relation

$$\frac{H_{\Delta\theta}}{H} = \cos\Delta\theta , \qquad (9)$$

where H is the wave height predicted in the last time step and $H_{\Delta\theta}$ is the reduced wave height due to the directional change of wind $\Delta\theta$, and the latter is used as the present wave height. IJIMA (1968) gave some physical meaning to the relation (9), based on the concept of directional spectrum. We will not enter deep into the physical basis of (9). It is justified only on the points that it is unity for $\Delta\theta=0$ and it is a monotonously decreasing function of $\Delta\theta$. In order to investigate empirically the effect of the functional form of the right hand side of (9) on the predicted values, the following relation

$$\frac{E_{\Delta\theta}}{E} = \cos^k\Delta\theta \qquad (10)$$

is used for the estimation of the reduced wave energy $E_{\Delta\theta}$ due to the directional change of wind. In the expression (10), k is a variable, and the case $k=2$ corresponds to the formula (9). In the examples shown in the next section,

the prediction is performed for each value of k equal to 0, 2 and 4, and the results are compared with one another.

2-3. Numerical procedures for swell

Even if (10) is used for the estimation of the effect of directional change of wind $\Delta\theta$, the relation cannot be considered appropriate for the case of lateral and adverse winds. In the present study, these cases are treated as follows. For the lateral wind case which is defined by $115°>|\Delta\theta|>65°$, the wave packet is assumed to propagate as swell in the same direction as that of the previous step. In addition, a new wave packet whose present energy is zero, is started in the new wind direction. As a result, the number of wave packets increases. For the adverse wind case which is defined by $180°\geqq|\Delta\theta|\geqq115°$, the wave packet is assumed to be extinguished, and a new wave packet whose present energy is zero is started in the new wind direction. In this case, the number of wave packets is not changed.

These procedures are not necessarily based on observed results. However, since there has been neither sufficient observational evidence nor adequate theoretical treatment for these cases, we have to rely on these somewhat arbitrary assumptions for the prediction of wind waves.

In addition to the lateral wind case, swells can appear in the cases of wind speed decrease and of fully developed wind waves. As a condition of defining swells and wind waves for such cases, we use Toba's (1978) criterion,

$$H^*>H_1^*\equiv BT_1^{*3/2}=242\,. \qquad (11)$$

When the inequality (11) is fulfilled, the waves are regarded as swells. The swells are assumed to propagate in the same direction as that of the previous step.

The prediction of the behavior of swells is also a weak point of the representative wave method. To overcome this problem, BRETSCHNEIDER (1968) proposed an empirical relation to express the damping process of swells which can be interpreted as a fetch graph of swells, that is,

$$\frac{H_D}{H_F}=\left[\frac{k_1F}{k_1F+D}\right]^{1/2}\equiv K_H\,, \qquad (12)$$

and

$$\frac{T_D}{T_F}=[k_2+(1-k_2)K_H]^{1/2}\,, \qquad (13)$$

where the variables with a suffix F represent the values at the time when the waves just become swells, those with D the values at the point separated by the distance D from the point where the waves just become swells, k_1 and k_2 are empirical constants, and F is the distance from the point from which the zero-energy wave packet was started up to the point where the waves just changed to swells. In the present article, these relations are used, with k_1 and k_2 as 0.4 and 2.0, respectively.

It should be noted that, in the present calculation, swells are assumed to redevelop as wind waves when the inequality (11) becomes unfulfilled. As a result, in some cases, a wave packet repeats wind-wave and swell states. In such a case, the fetch F in the relation (12) is defined as the total distance of propagation of the wave packet as wind waves.

2-4. Drag coefficient of wind

In the basic equations such as (1) and (3), u_* is used as the scale factor of the wind speed. On the other hand, the wind data available for the wave prediction is generally in the form of U_{10} or $U_{19.5}$, i.e. the wind speed at the height 10 m or 19.5 m, respectively. To convert the given wind speed to the friction velocity u_*, the drag coefficient of wind C_D must be known. As reported by many investigators, C_D depends at least on the wind speed. WU (1969) reported the dependence of C_{D10} on U_{10} in m s^{-1} for wind speeds up to 30 m s^{-1}, as

$$\left.\begin{aligned} &C_{D10}=0.5\times3^{1/2}\times10^{-3},\ U_{10}<3,\\ &C_{D10}=0.5\times U_{10}^{1/2}\times10^{-3},\ 3\leqq U_{10}\leqq15,\\ &C_{D10}=2.6\times10^{-3},\ 15<U_{10}<30. \end{aligned}\right\} \qquad (14)$$

Although there was no division at $U_{10}=3$ m s^{-1} in the original paper by WU, we add it considering other reports. The drag coefficient C_{Dz} at any height z (m) can be calculated from C_{D10} by the relation

$$C_{Dz}=\left[\frac{1}{\kappa}\ln\frac{z}{10}+C_{D10}^{-1/2}\right]^{-2}, \qquad (15)$$

where κ is von Kármán constant equal to 0.4. With the relation (15), $C_{D19.5}$ is given from (14) and approximated with a functional form

$$\left.\begin{aligned} C_{D19.5}&=(0.075+0.4\times 3.15^{1/2})\times 10^{-3}, \\ &\qquad U_{19.5}<3.15\,, \\ C_{D19.5}&=(0.075+0.4\times U_{19.5}{}^{1/2})\times 10^{-3}, \\ &\qquad 3.15\leqq U_{19.5}\leqq 16.1\,, \\ C_{D19.5}&=2.2\times 10^{-3}, \\ &\qquad 16.1<U_{19.5}<32.6\,. \end{aligned}\right\} \quad (16)$$

where $U_{19.5}$ is in m s^{-1}. Since the maximum wind speed in the example of the next section is about 30 m s^{-1}, the relation (14) or (16) can be used in the present study. However, the relations have a discontinuity in C_D at 15 m s^{-1} of U_{10} or at 16.1 m s^{-1} of $U_{19.5}$, and it might have undesirable effects on the numerical results. To check it, another functional form of

$$C_{D10}=(1+0.07\times U_{10})\times 10^{-3} \quad (17)$$

is also used and the results are compared. Although the form (17) is proposed by DEACON and WEBB (1962) only for the wind speed up to 15 m s^{-1} of U_{10}, it is used with the assumption that the form (17) is valid up to 30 m s^{-1}. As a converted form of (17) into $C_{D19.5}$,

$$C_{D19.5}=(0.92+0.052\times U_{19.5})\times 10^{-3} \quad (18)$$

is used for the study. The two equations (14) and (17) are compared in Fig. 1 for the clarification of their differences.

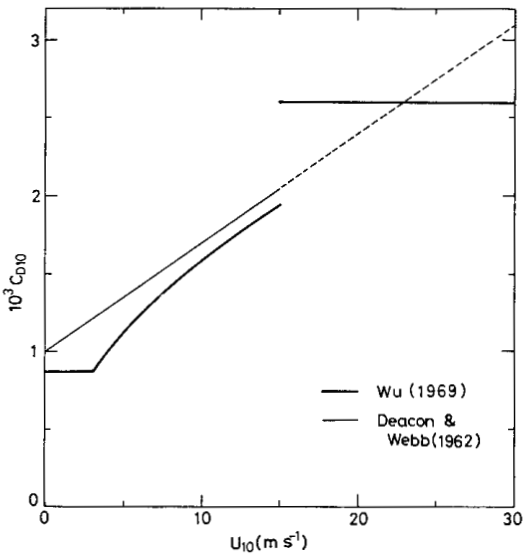

Fig. 1. A comparison of the two forms of C_{D10} proposed by different authors stated in the figure.

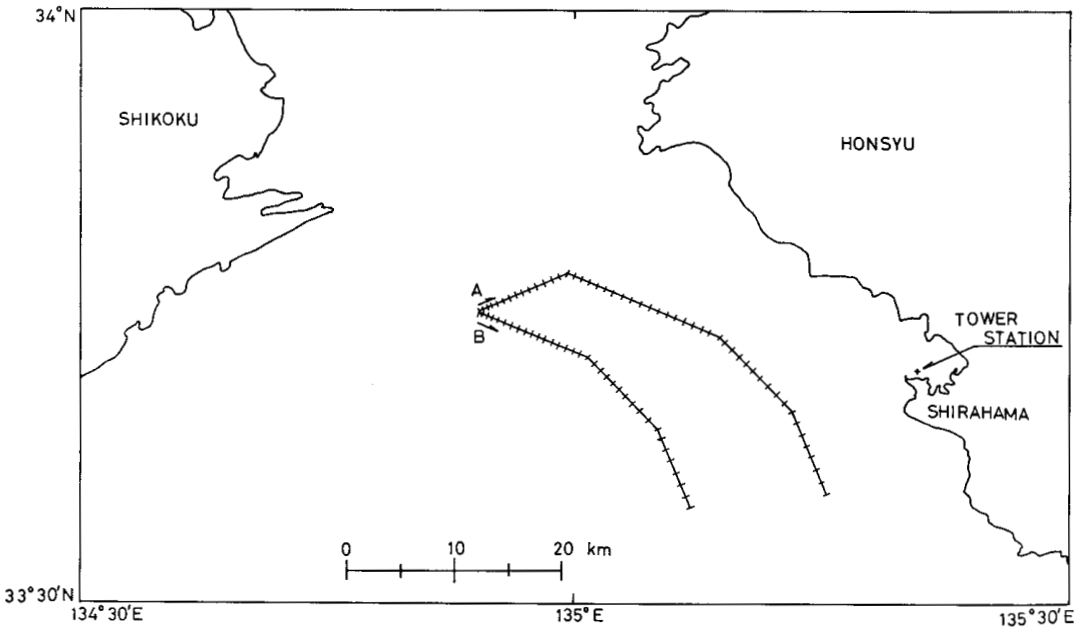

Fig. 2. Location of the Shirahama Oceanographic Tower Station in Kii Channel Approach. Examples of simultaneous wave-packet paths are shown for two paths starting from the same point.

3. Examples

In this section, two examples are taken to test the present method of ocean-wave prediction, one corresponds to the waves in a small scale area and the other to the waves in a large scale area.

3-1. Small scale case

The wave data observed by TOBA *et al.* (1971) at the Shirahama Oceanographic Tower Station of Kyoto University is hindcasted, as an example to test the present method in a relatively small scale area. Since the observation and its results were reported in detail by TOBA *et al.* (1971) and by KAWAI *et al.* (1977), only its outline will be described. The observation was performed on November 10, 1969 at the tower station located near the east coast of Kii Channel Approach as shown in Fig. 2. In Fig. 3, the weather map 7 hours before the beginning of the observation is given. The cold front shown in the figure crossed the tower station at about 9:00 a.m., then the winter monsoon started to blow.

In the prediction, the wind speed U_{10} observed at the tower station is assumed to be homogeneous in the entire region, though temporally changing. This assumption seems to be reasonable, since the region related to the prediction is not so large, as will be shown later. The time interval Δt of numerical integration is set to be 1/8 hour. Since the wind is homogeneous, a graphic method can be partially used, as follows, and the graphic method makes easier treatment of complicated coast lines. At first, a wave packet with zero-energy is started from a point in an ideal sea which has no coast, and the consecutive behavior of the wave packet driven by the wind is calculated with the method described in the previous section. Similar wave packets are started at intervals Δt from the original point in the ideal sea, and similar calculation is performed for each packet. These calculations give the path lines of each packet. These path lines are drawn to the scale of the chart of Fig. 2, on separate transparent papers. The path drawings are placed over the chart and moved parallel to the latitude or longitude of the location chart so as to make the position of a wave packet for a particular time step coincide with the tower station. When the position hits the tower point, a search is made to see whether or not the path line is touching the coast at any place. If it is not touching coast, the wave characteristics are noted. This is repeated for all paths and the maximum value for that particular time step is taken as the significant wave height and period at the tower station for that particular time step. Similar procedures are performed for every time step. As examples, two path lines are drawn in Fig. 2. The wave packet A is started at 9:52.5 and B started at 11:52.5. The short cross lines are entered at every Δt hours, and the last one represents 16:07.5 which corresponds to the end of observation. From the figure, the east-west scale of the region relating to the phenomena is estimated to be about 30 km.

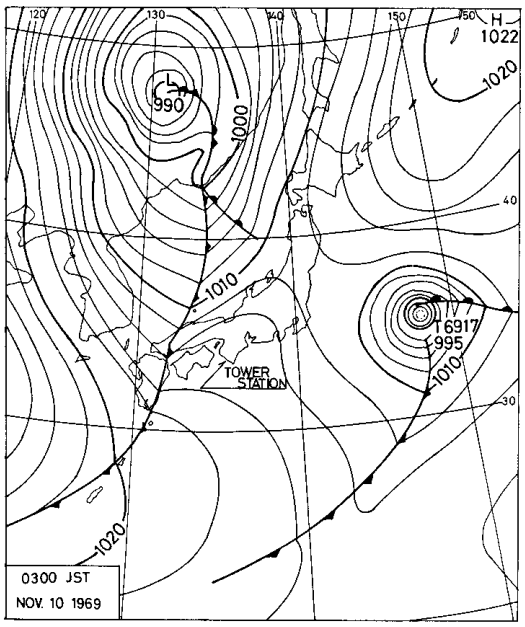

Fig. 3. Weather map observed 7 hours before the obervation at the Tower Station.

Fig. 4 shows a comparison between the calculated and observed values, for the case where the value of k in (10) is 4 and (14) is used for C_{D10}. In the figure, the observed wind is also represented. The calculated values represent the observed growth process of wind waves well. For the case of $k=2$ shown in Fig. 5, the calculated values rather overestimate the wave height and period, although they represent the overall trend of observed values.

3-2. Large scale case

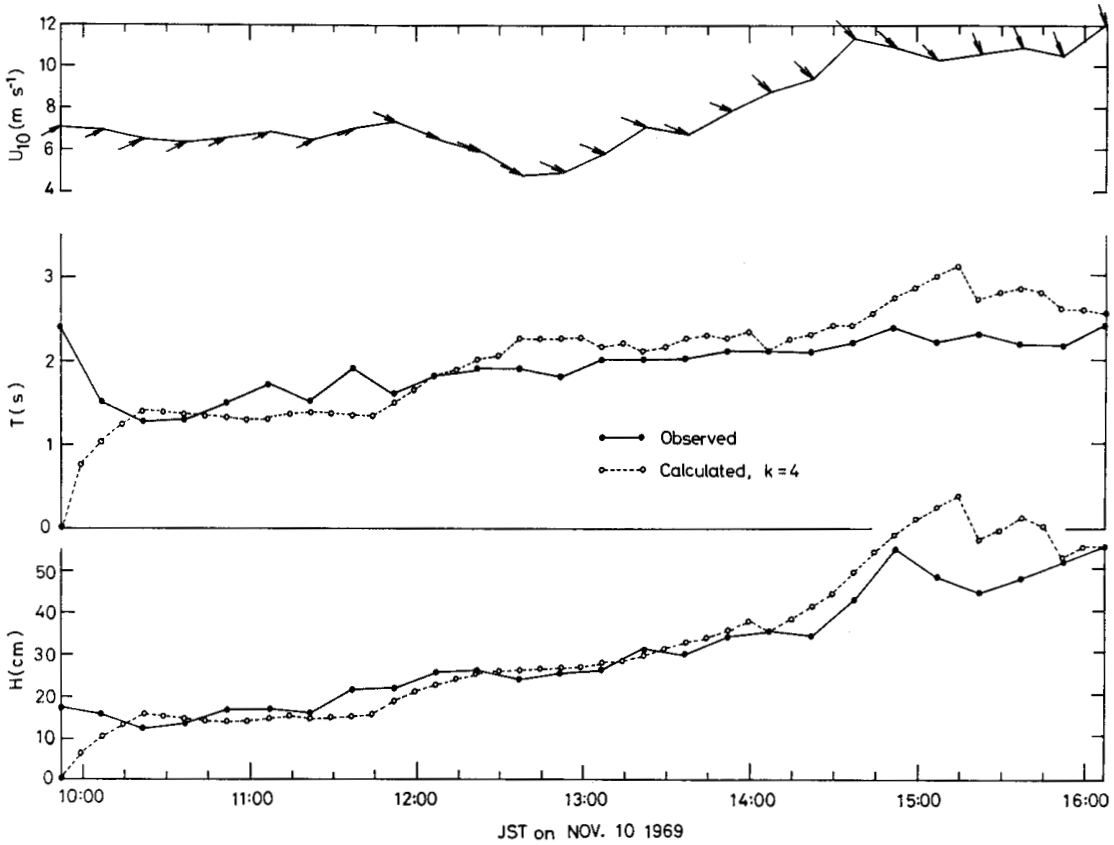

Fig. 4. A comparison of the wave characteristics between the observed value and the calculated value with the condition C_{D10} by (14) and $k=4$, for the Kii Channel case. Observed values of wind speed U_{10} and direction (arrows) are also shown.

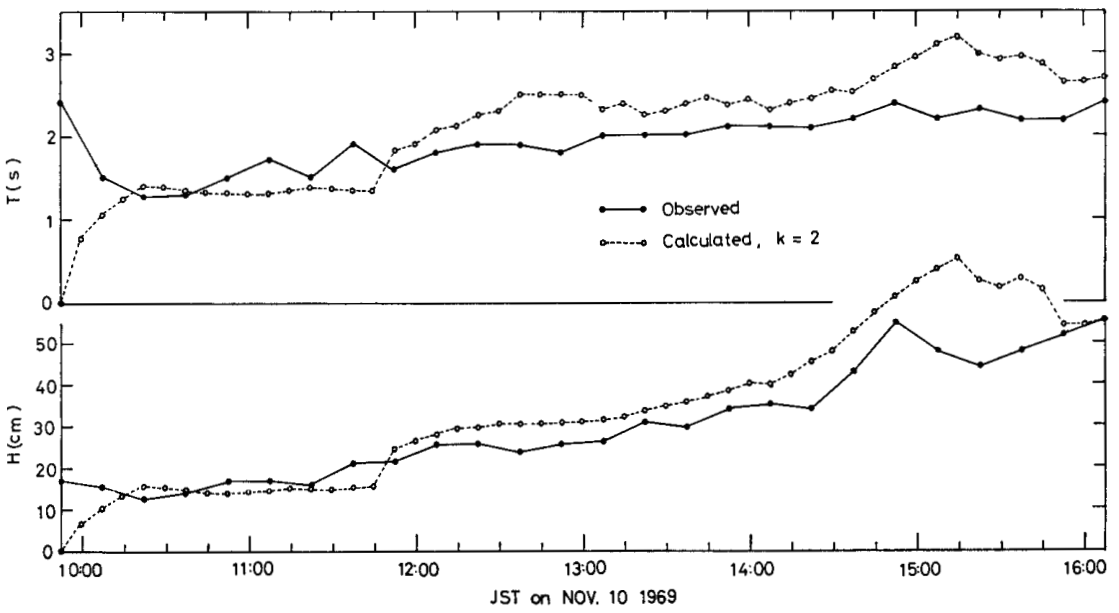

Fig. 5. As in Fig. 4, except for $k=2$.

A number of numerical methods for predicting ocean waves have been tested with the available data of the North Atlantic Ocean of December 1959, whose wind and wave conditions were reported in detail by BRETSCHNEIDER *et al.* (1962). As an example of the large scale case, the present method has to be tested with the same data, for comparison of results with other methods. The data of wind speed $U_{19.5}$ and the direction θ prepared by ISOZAKI and UJI (1973) with an objective analysis of atmospheric pressure data of the above region, was used through the courtesy of Dr. ISOZAKI. The original data supplied by ISOZAKI and UJI did not contain coastal values, since their model does not depend on them. In our case it is assumed that the coastal values are equal to those at the nearest point in the sea. Since the present calculation is made with a time interval Δt of 1 hour, the required wind data were prepared by vector interpolation of the original 6-hour interval data. The region considered for the present study is shown in Fig. 6, where the thick lines represent the coast of the present numerical model and the dots represent the points having original wind data.

In the present wave-packet following method, the prediction is performed by following the wave packets which are driven by wind, and the wave packets may propagate to positions where no wind data is given. In the present study the wind data are given only at the grid points shown in Fig. 6. As a result, two problems are encountered, firstly wind data have to be acquired at arbitrary points, secondly some adequate measures have to be taken for prediction at a fixed point. The former is solved by a spatial vector interpolation, as shown in Appendix. Although in the previous example, the latter problem was solved by a graphic treatment, it cannot be applied to the present problem where the wind changes spatially. In the present example, the following method is used for simplicity and reduction of computer time. As shown in Fig. 7, a sub-region containing the required point (J in the example) is taken in the analyzed region. For each wave packets which pass through the sub-region, the quantities at the point nearest to J in the path line is assumed to represent those, at J at the time when the packet remains at the nearest point. Shape and scale of the subregion should be decided according to the requirements of accuracy and resolving power for the results. In the present case, the sub-region is selected as a square with sides equal to twice the grid size, being equivalent to four unit squeres of the grid, as shown in the figure.

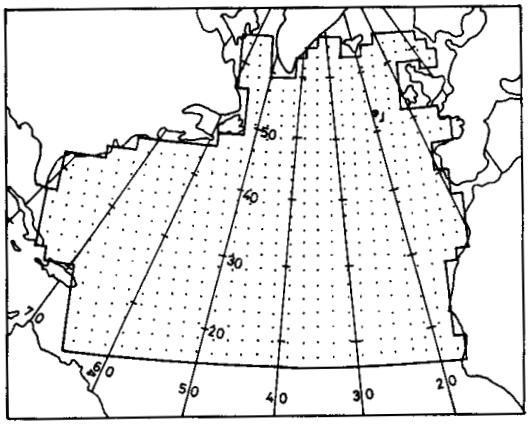

Fig. 6. Location of the weather ship point J in the analyzed area of the Atlantic case. Thick line is the numerical coast, and dots for the points with original wind data by ISOZAKI and UJI (1973).

The calculation is started on December 10, and the calculated values are compared with the observation for December 16 through 20, as done by ISOZAKI and UJI (1973). For the standard calculation, (16) is used for $C_{D19.5}$ and k in (10) is set to 4. The prediction for fixed point with the method described above is given only for a single point J of the Ocean Weather Ship shown in Fig. 6.

Fig. 8 shows the result of the standard case

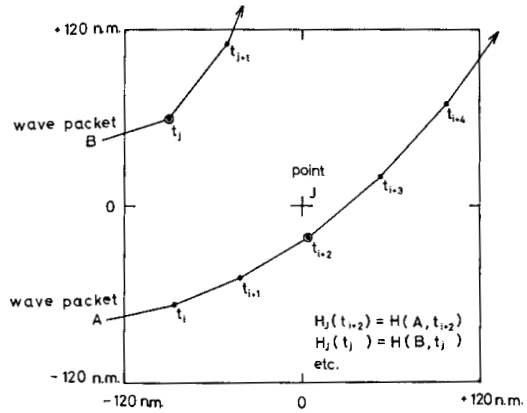

Fig. 7. Definition sketch to decide the wave height at the point J. (See the context.

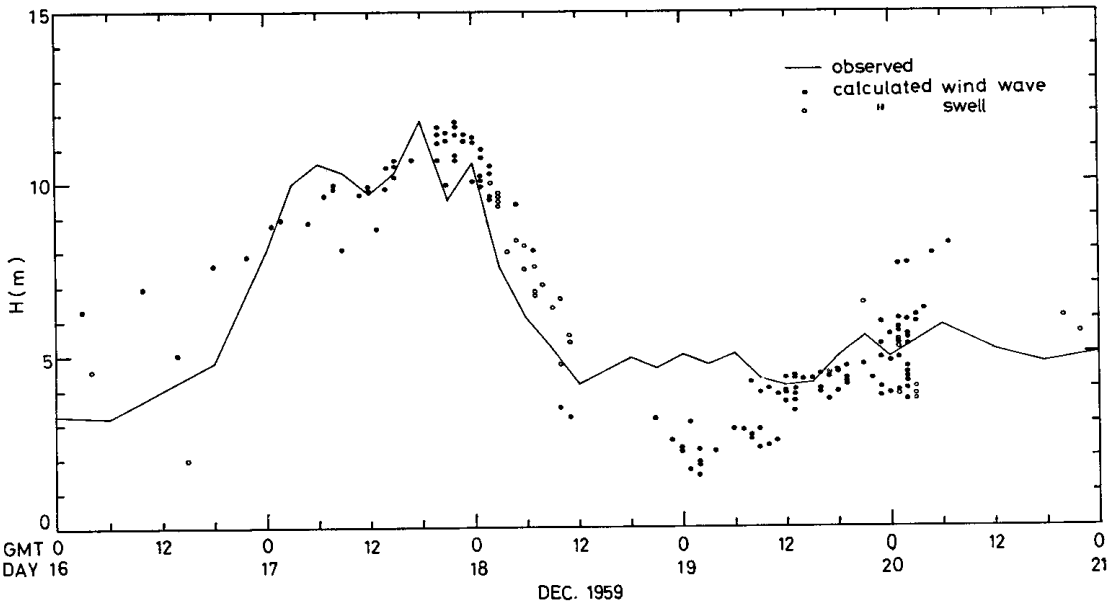

Fig. 8. A comparison of the wave height between the observed value and the calculated value with the condition $C_{D19.5}$ by (16) and $k=4$. Wave packets are started from the coastal points at 10D00Z through 20D18Z.

where zero-energy wave packets are originating at grid points on the numerical coast line. They are started every 6 hours from 00GMT on December 10, which is hereafter described as 10D00Z, up to 20D18Z. The solid circles show the packets which hit the point J in the state of wind waves, and the open circles for those as swells. The calculated values generally agree with the observed values which are shown by a solid line.

However, the density of the calculated points changes with time, and at certain times nearly blank regions appear. The inequality of the data density is inherent in the present wave-packet following method, in which the path lines of wave packets are wholly controlled by the wind, and wave packets are scanty in the region where the wind diverges. To overcome the problem, new wave packets have to be entered at the region of diverging wind. Instead of searching such a region, new wave packets are started from every inner grid points in the present study, to investigate the effect of the entrance of the new packets. The wave energy of the new packets at the start is taken as zero, for the simplicity of the computer program. We have to be careful of the fact that it is not entirely reasonable to assume that the energy at the inner grid point to be zero, although it is real at the coast line. To minimize the effect of these rather inappropriate procedures, new wave packets were entered before the interval of the comparison with the observed values. Fig. 9 shows the results, where the symbols are same as in Fig. 8. As in WILSON (1955), it is now assumed that the envelope of those predicted points represents the most probable estimation of wave height. With this assumption, there is no notable change in Fig. 9 from Fig. 8. Therefore, in general, the wave packets started at the coast line may accurately predict the wave height.

The predicted values are compared with those of other models in Fig. 10. Two predicted values are shown in the figure for the present calculation, of which one represents the value based on the envelope as described above, and the other represents the mean value, which will be described in detail in the next section. In the remaining part of this section, a discussion based on the former values will be made. The predicted values in Fig. 10 were calculated with the spectrum method except those of WILSON (1965) and of the present case. It is noticeable

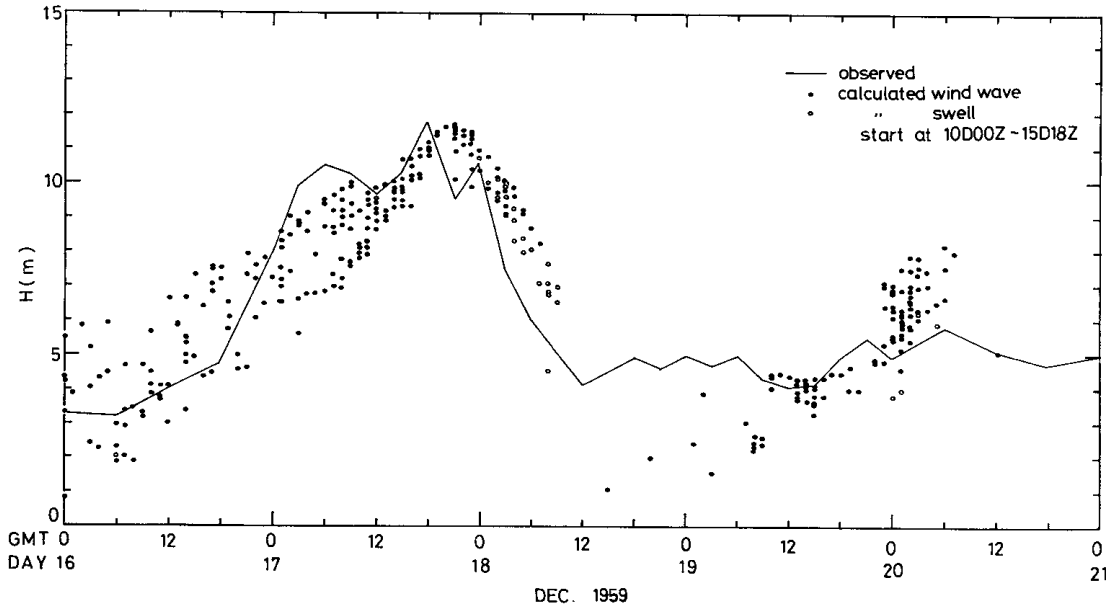

Fig. 9. As in Fig. 8, except for wave packets started from the inner points at 10D00Z through 15D18Z.

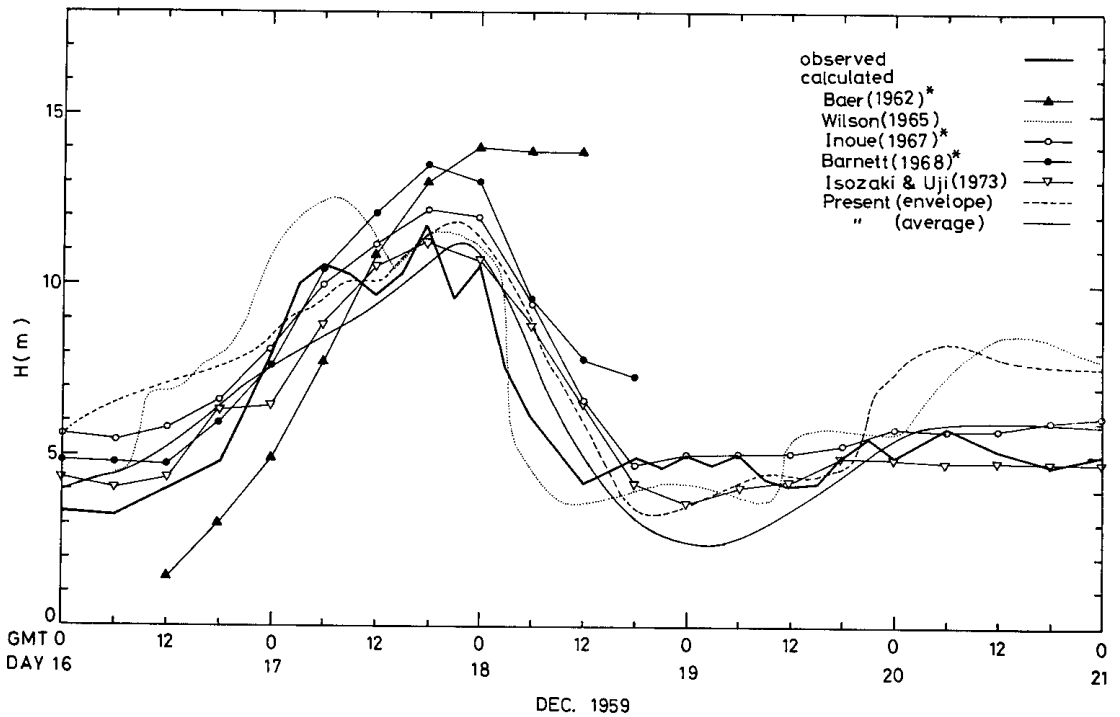

Fig. 10. Comparisons of the wave height between the observed values and the calculated values by various models. The results with a mark * are cited from ISOZAKI (1978).

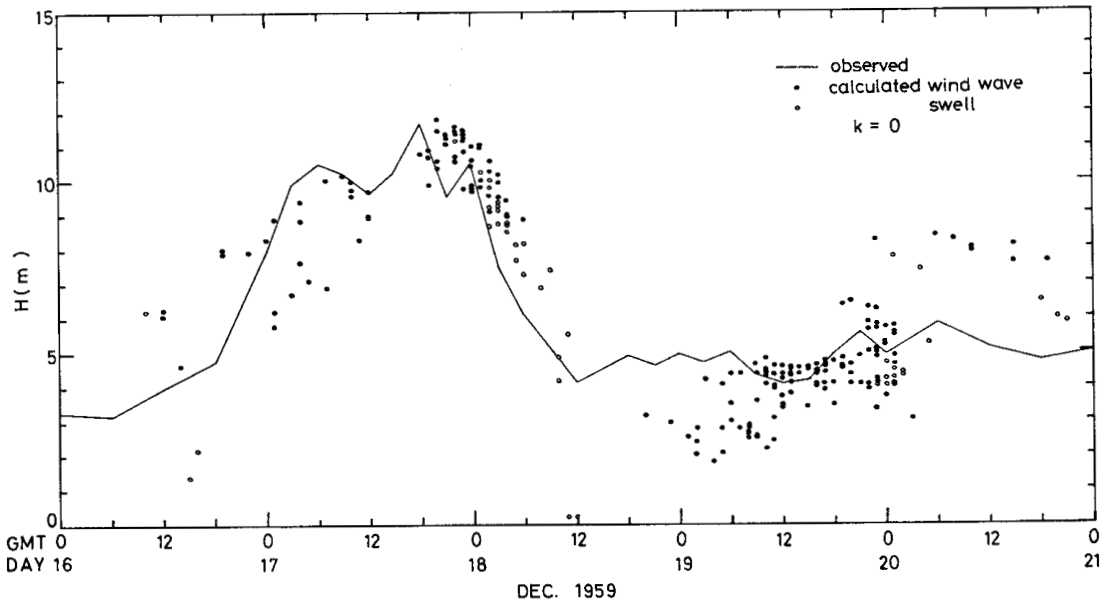

Fig. 11. As in Fig. 8, $k=0$.

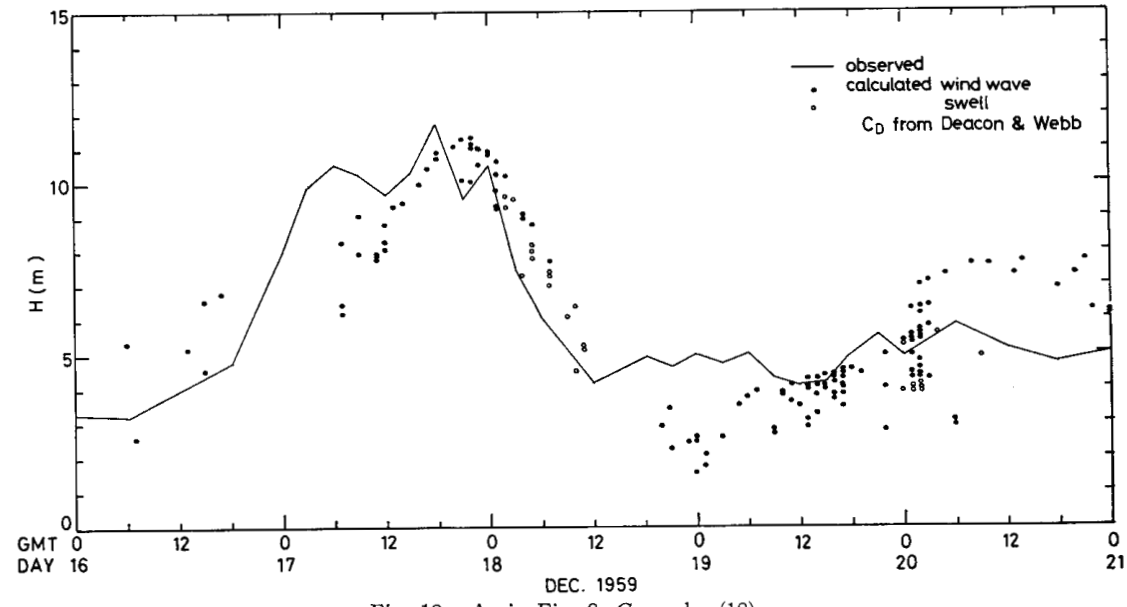

Fig. 12. As in Fig. 8, $C_{D19.5}$ by (18).

that, on the 16th and 20th days, the values for the present case are larger than the observed values and the values predicted by the spectrum method. Since a similar trend is also seen in the values predicted by WILSON (1965), it might be attributed to some undesirable factor common to the representative wave method. This point will be discussed later.

Next, the dependence of the present results on the parameters k in (10) and C_D is discussed. Fig. 11 shows the result with $k=0$, but with all other conditions the same as those of Fig. 8. The result shows minute changes from that in Fig. 8 and a similar result is also obtained for the case $k=2$, but is not shown in this paper. They show that the present method is nearly

independent of k for the present large scale case. This conclusion is opposite to that of the small scale case. This will also be discussed later.

Fig. 12 shows the result with $C_{D19.5}$ definded by (18), but with all other conditions the same as those of Fig. 8. The result shows minute changes from that in Fig. 8, and they show that the difference in the values of C_D given by (16) and (18) has no substantial effect on the results of the present method. In this connection, it should be noted that a simple model with a constant value of C_D irrespective of the wind speed, which was tested prior to the present model, failed to predict accurately the developing process of wind waves. Therefore, such a rather fine difference in the values of C_D as shown in Fig. 1 has no substantial effect on the results of the present method, but it does not mean the complete independence of the results from the functional forms of C_D.

In the present example where deep low pressures with fronts travel successively, the wind field is strongly two-dimensional. The present results show that the present method based on the representative wave concept is efficient even for these conditions.

4. Discussion

We shall first discuss the cause of the difference in the dependence of the numerical results on k, for the small and large scale cases. It seems that there are two reasons for their independence of k for the case of the North Atlantic Ocean. The first is that the directional change of the wind is small, and the second is that the time scale considered in the problem is large. As a result of the latter reason, the effect of a directional change of wind at a certain point, however large it may be, disappears in such a large time scale. About the former, the actual values of the angle change are at most 25°, and smaller than 5° for most cases. In contrast, for the case of Kii Channel Approach the maximum time scale is 6 hours, and the maximum directional change of wind is 45°.

From the above discussion, it seems that the relation of the maximum difference of angle $\Delta\theta_m$ to the time interval Δt, that is, $\Delta\theta_m=25°$ in $\Delta t=1$ hour for the Atlantic case and $\Delta\theta_m=45°$ in $\Delta t=1/8$ hour for the Kii Channel case, indicates that the very small scale changes of wind are well documented in the Kii Channel case but not in the Atlantic case. If we look at the properties of wind data, the original wind data in the Atlantic case were prepared every 6 hours and every 120 n.m. by an objective analysis of the weather maps, and the original data were interpolated spatially and temporally, according to the progress of the wave packets. As a result, the wind data has no information on local wind variations, and represents only a general situation. On the other hand, for the Kii Channel case, the original data were prepared by a time series of the observed values at every 15 minutes at the tower station, and they represent the local situation.

As can be recognized from the above discussion, the most suitable value of k for the present method depends on the scale of the problem and the nature of wind data. However, since in practices of prediction, the wind data is prepared by use of weather maps, whether observed or predicted, and the predicting interval is 1 hour or more, they are close to the present Atlantic case, and consequently, the predicted values are independent of k, or in other words, we may take the value k as zero. As a result, for the general situation wind waves may be considered to propagate in the local wind direction, conserving their total energy.

Next, we discuss the reasons for the overestimate of wave height on the envelope of the predicted values on the 16th and 20th days for the Atlantic case. It is noticeable that the individual predicted values on these days, scatter more widely than on other days. Since this scatter can be seen even in Fig. 8 where the unnatural entrance of zero-energy wave packets was not made, the disagreement and the scattering of the predicted values are not caused by this unnatural procedure. To clarify the reason for the scatter, the spatial distribution of the wave heights at 20D00Z in Figs. 8 and 9 is shown in Fig. 13. The figure shows that the wave heights distribute spatially not at random but somewhat in order. The wave height is higher near the point J, decreases southward, and lower swells exist in the northern portion. The reason is not yet explained. However, some consideration is necessary to interpret the

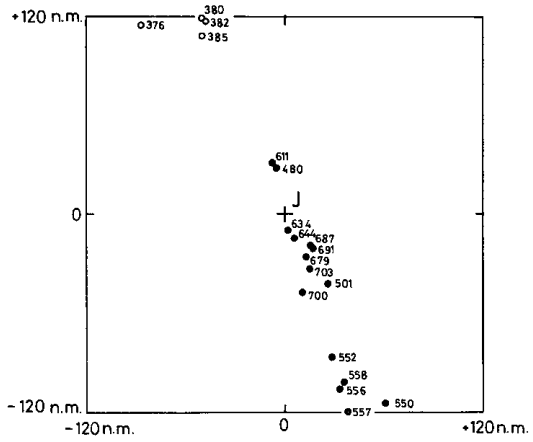

Fig. 13. Calculated distribution of wave heights, in cm, at 20D00Z. Solid circles show wind waves, and open circles swells.

wave heights, when there is such conspicuous distribution of wave heights in a sub-region near the considered point. Although the wave packets are assumed to be independent of the other wave packets in the present wave-packet following method, the real process might have a trend to make the distribution of wave heights uniform, especially in such a case where the energy concentrates in a narrow region as shown in Fig. 13. Therefore, the distribution in Fig. 13 is not realized, but a more uniform distribution might be realized. As a simple method to obtain the more uniform distribution, we will use a mean value of the individual wave heights in Figs. 8 and 9, to represent the wave height at the point J. The result is shown also in Fig. 10 with a thin solid line. The average value and the standard deviation of the error ΔH of the predicted wave height, which is defined by its difference from the observed value, are

$$\overline{\Delta H}=1.20\ \text{m},\ \sigma_{\Delta H}=1.61\ \text{m}, \quad (19)$$

for the envelope values of the predicted wave heights and

$$\overline{\Delta H}=-0.02\ \text{m},\ \sigma_{\Delta H}=1.33\ \text{m}, \quad (20)$$

for the mean values of the predicted wave heights in Figs. 8 and 9. Comparison of (19) and (20) shows that the latter predicted value is more accurate than the former. As a result, we may conclude that, if we use the mean value of the predicted values for the wave packets, the present method can predict the wave height with a standard deviation of 1.3 m for waves with wave heights in the range of 3 to 12 m.

To conclude, we will discuss a possible improvement of the present method. Above, we have seen that the present wave-packet following method may give unnatural energy concentration. This undesirable tendency resembles, though the sense is opposite, to the tendency of much energy dispersion seen in the spectrum method that uses a simple adaptation of a finite difference method. In the model by PIERSON *et al.* (1965) which belongs to the spectrum method, this tendency was minimized by the "jumped" technique, where the energy of a component wave remains at a particular grid point until enough time has elapsed so that the energy could reach the vicinity of a neighboring grid point. A similar technique was also used in the model by UJI and ISOZAKI (1972). The essential point of these techniques is to weaken the strong coupling between adjacent points inherent in the finite difference methods, using a method similar to the wave-packet following method where wave packets are fully independent of each other. Similarly, in order to minimize the unnatural concentration of energy in the present method, we can use a compromise where the wave-packets properly interact. One of the possible ways is as follows. Wave packets are initially distributed on the grid points such as those in Fig. 6, and their energy contents are given. When the situation is settled, the energy and the position obtained by these wave packets after the interval Δt are predicted by the present wave-packet following method. Then, we can calculate the wave energy on the original grid points through a spatial interpolation of the predicted values. For the calculation in the next time interval, these values at the grid points are used as the initial values. In such a procedure, wave packets interact with each other. This compromise has a simultaneous merit in that it can provide the time sequence of the predicted values directly at prescribed points. It is now being developed, and the results will be shown in a succeeding paper.

Acknowledgements

The authors express their deep thanks to Dr. I. ISOZAKI of the Meteorological Research Institute, Japan Meteorological Agency, for his kindness in lending them the wind data for the Atlantic. They also thank Prof. H. MITSUYASU of Kyushu University for comments on the original manuscript. This study was performed partially as a member of Commission of Development of Ocean-wave Prediction Techniques, which was organized within the Japan Weather Association in August, 1978. The computation contained in the present article was performed by use of ACOS-NEAC-700 at the Computer Center of Tohoku University.

Appendix

To explain the numerical scheme, the basic equation (6) is transformed into a symbolical form

$$\frac{d\tilde{E}}{dt^*}=G_0R[1-\mathrm{erf}(b\tilde{E}^{1/2})]\equiv f_E(\tilde{E}), \quad \text{(A1)}$$

where $\tilde{E}$ is defined by

$$\tilde{E}=E^{*2/3} \quad \text{(A2)}$$

and hereafter it is also called energy. When the energy $\tilde{E}_i$ at a time t_i is given, the energy $\tilde{E}_{i+1}$ at $t_i+\Delta t$ is calculated with an iteration scheme as follows,

$$\tilde{E}_{i+1}^{(n)}=\tilde{E}_i+f_E(\tilde{E}_i^{(n)})\Delta t^*,\ n\geqq 0, \quad \text{(A3)}$$

where (n) is the number of iterations, and

$$\tilde{E}_i^{(0)}=\tilde{E}_i, \quad \text{(A4)}$$

$$\tilde{E}_i^{(n)}=(\tilde{E}_{i+1}^{(n-1)}+\tilde{E}_i)/2,\ n\geqq 1, \quad \text{(A5)}$$

$$\Delta t^*=g\Delta t/u_*. \quad \text{(A6)}$$

The final value $\tilde{E}_{i+1}$ is defined by

$$\tilde{E}_{i+1}=\tilde{E}_{i+1}^{(n)},\ \text{if}\ \left|\frac{\tilde{E}_{i+1}^{(n)}-\tilde{E}_{i+1}^{(n-1)}}{\tilde{E}_{i+1}^{(n-1)}}\right|\leqq\varepsilon, \quad \text{(A7)}$$

where ε is a small value and set as 10^{-4} in the present study. From the definition (A2), there is a relation between $\tilde{E}_{i+1}$ and the dimensional energy E_{i+1}, as

$$\tilde{E}_{i+1}=\left(\frac{g^2E_{i+1}}{u_*^4}\right)^{2/3} \quad \text{(A8)}$$

Wave height H_{i+1} is calculated from E_{i+1} with the relation

$$E_{i+1}=H_{i+1}^2/16, \quad \text{(A9)}$$

which is a repetition of (2). Wave period T_{i+1} is calculated from H_{i+1} with the relation

$$\frac{gH_{i+1}}{u_*^2}=B\left(\frac{gT_{i+1}}{u_*}\right)^{3/2}, \quad \text{(A10)}$$

which is a repetition of (1). The distance ΔF_i progressed by the wave packet in Δt is calculated, using the relations (7) and (8), by

$$\Delta F_i=\frac{1}{2}\frac{g}{2\pi}\frac{T_i+T_{i+1}}{2}\Delta t. \quad \text{(A11)}$$

Based on the definition sketched in Fig. 14 the components of the distance is defined by

$$\left.\begin{aligned}\Delta x_i&=\Delta F_i\cos\theta_i,\\ \Delta y_i&=\Delta F_i\sin\theta_i.\end{aligned}\right\} \quad \text{(A12)}$$

We will explain, next, how $\tilde{E}_i$ in (A3), (A4) and (A5) is calculated. With the definition in Fig. 14, it is defined by

$$\left.\begin{aligned}\tilde{E}_i&=\left(\frac{g^2E_i}{u_*^4}\cos^k\Delta\theta_i\right)^{2/3},\ \text{if}\ |\Delta\theta_i|\leqq 65^\circ,\\ \tilde{E}_i&=0,\qquad\qquad \text{if}\ 65^\circ<|\Delta\theta_i|\leqq 180^\circ,\end{aligned}\right\} \quad \text{(A13)}$$

where k is the variable defined in (10). For the case $65^\circ<|\Delta\theta_i|<115^\circ$, swells with wave height H_i and period T_i also propagate to the direction θ_{i-1}. Swells appear also in the case where the

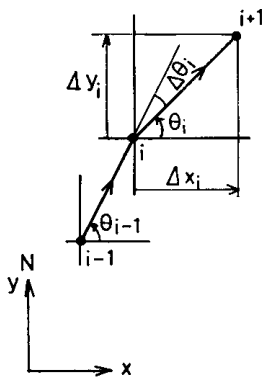

Fig. 14. Sketch to explain the wave-packet following method. (See the context.)

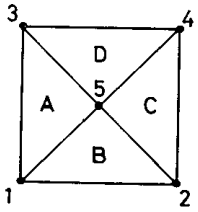

Fig. 15. Sketch to explain the spatial mean method of vector variables. (See the context.)

inequality (11) is fulfilled.

Finally, we will explain the calculation of the value u_*. Although the suffix i is removed in the above explanation, the friction velocity u_{*i} in (A6), (A8), (A10) and (A13) is that at the time t_i, and it is calculated from the wind velocity U_i with the relation

$$u_{*i}=C_D^{1/2}U_i\,. \qquad \text{(A14)}$$

To estimate the wind velocity at arbitrary points, a vector interpolation method is used. With the definition in Fig. 15, the wind vectors at the points 1 through 4 are given, and that at 5 is calculated by the vector mean. If the point considered lies in the triangle A, the wind vector at the point is calculated from those at the points 1, 3 and 5 with linear interpolation. For the other cases the calculation is performed in a similar way.

References

BARNETT, T.P. and K.E. KENYON (1975): Recent advances in the study of wind waves. Rep. Prog. Phys., **38**, 667-729.

BRETSCHNEIDER, C.L. (1968): Fundamentals of ocean engineering—Part 8. Decay of wind generated waves to ocean swell by significant wave method. Ocean Industry, March, 36-39 and 51.

BRETSCHNEIDER, C.L., H.L. CRUTCHER, J. DARBYSHIRE, G. NEUMANN, W. J. PIERSON, H. WALDEN and B.W. WILSON (1962): Data for high wave conditions observed by the OWS "Weather Reporter" in December 1959. Deut. Hydrogr. Zeit., **15**, 243-255.

DEACON, E.L. and E.K. WEBB (1962): Interchange of properties between sea and air. Ch. 3. Small-scale interaction. *In*, The Sea, Vol. 1, edited by M.N. HILL, Interscience, N.Y., pp. 43-87.

HASSELMANN, K., T.P. BARNETT, E. BOUWS, H. CARLSON, D.E. CARTWRIGHT, K. ENKE, J.A. EWING, H. GIENAPP, D.E. HASSELMANN, P. KRUSEMAN, A. MEERBURG, P. MÜLLER, D.J. OLBERS, K. RICHTER, W. SELL and H. WALDEN (1973): Measurements of wind-wave growth and swell decay during the Joint North Sea Wave Project (JONSWAP). Deut. Hydrogr. Zeit., Suppl. A, 8, No. 12, 95 pp.

HASSELMANN, K., D.B. ROSS, P. MÜLLER and W. SELL (1976): A parametric wave prediction model. J. Phys. Oceanogr., **6**, 200-228.

IJIMA, T. (1968): Numerical prediction of waves. Text for The Seminar on Advanced Hydraulics and Hydraulic Engineering, A-course, pp. 2-1 to 2-30, JSCE, Tokyo. (in Japanese)

IJIMA, T., T. SOEJIMA and T. MATSUNO (1967): On the distribution of waves in a typhoon area estimated by a numerical calculation — a case of typhoon over ocean —. Proc. 14th Conf. Coastal Engineering in Japan, pp. 29-38 (in Japanese).

ISOZAKI, I. (1978): Recent progress in ocean waves prediction and some problems for its further advances. Umi to Sora, **53**, 47-60 (in Japanese with English abstract and figure captions).

ISOZAKI, I. and T. UJI (1973): Numerical prediction of ocean wind waves. Pap. Met. Geophys., **24**, 207-231.

KAWAI, S. (1979): Generation of initial wavelets by instability of a coupled shear flow and their evolution to wind waves. J. Fluid Mech., **93**, 661-703.

KAWAI, S., K. OKADA and Y. TOBA (1977): Field data support of three-seconds power law and $gu_*\sigma^{-4}$-spectral form for growing wind waves. J. Oceanogr. Soc. Japan, **33**, 137-150.

LONGUET-HIGGINS, M.S. (1952): On the statistical distribution of the heights of sea waves. J. Mar. Res., **11**, 245-266.

MILES, J.W. (1957): On the generation of surface waves by shear flows. J. Fluid Mech., **3**, 185-204.

MILES, J.W. (1962): On the generation of surface waves by shear flows, Part 4. J. Fluid Mech., **13**, 433-448.

MITSUYASU, H., F. TASAI, T. SUHARA, S. MIZUNO, M. OHKUSU, T. HONDA and K. RIKIISHI (MS): Observation of the power spectrum of ocean waves using a cloverleaf buoy. (submitted to J. Phys. Oceanogr.)

OKUDA, K. (MS): Internal structure of wind waves. (in preparation)

PHILLIPS, O.M. (1957): On the generation of waves by turbulent wind. J. Fluid Mech., **2**, 417-445.

PIERSON, W.J., L. TICK and L. BAER (1965): The accuracy and potential uses of computer based wave forecasts and hindcasts for the North Atlantic. Proc. Second Military Oceanogr. Symp., **1**, 69-82.

SVERDRUP, H.Y. and W. MUNK (1947): Wind, sea and swell. Theory of relations for forecasting.

Publ. No. 601, U.S. Hydrogr. Office, Washington, D.C, 44 pp.

TOBA, Y. (1972): Local balance in the air-sea boundary processes. I. On the growth process of wind waves. J. Oceanogr. Soc. Japan, **28**, 109-121.

TOBA, Y. (1978): Stochastic form of the growth of wind waves in a single-parameter representation with physical interpretations. J. Phys. Oceanogr., **8**, 494-507.

TOBA, Y., H. KUNISHI, K. NISHI, S. KAWAI, Y. SHIMADA and N. SHIBATA (1971): Study of the air-sea boundary processes at the Shirahama Oceanographic Tower Station. Disaster Prevention Res. Inst., Kyoto Univ., Annals, **14B**, 519-531 (in Japanese with English abstract and figure captions).

TOBA, Y., M. TOKUDA, K. OKUDA and S. KAWAI (1975): Forced convection accompanying wind waves. J. Oceanogr. Soc. Japan, **31**, 192-198.

TOKUDA, M. and Y. TOBA (MS): Similarity for individual waves in wind-wave field under strong coupling with the wind. (to be submitted to J. Phys. Oceanogr.)

UJI, T. and I. ISOZAKI (1972): The calculation of wave propagation in the numerical prediction of ocean waves. Pap. Met. Geophys., **23**, 347-359.

WILSON, B. W. (1955): Graphical approach to the forecasting of waves in moving fetches. B.E.B. Tech. Memo., No. 73, 31 pp.

WILSON, B. W. (1961): Deep water wave generation by moving wind system. Proc. ASCE, **87**, No. WW2, pp. 113-141.

WILSON, B. W. (1965): Numerical prediction of ocean waves in the North Atlantic for December 1959. Deut. Hydrogr. Zeit., **18**, 114-130.

WU, J. (1969): Wind stress and surface roughness at air-sea interface. J. Geophys. Res., **74**, 444-454.

風波の単一パラメータ発達方程式に基づく海洋波浪の予測

河合三四郎*, Paimpillil S. JOSEPH*, 鳥羽良明*

要旨: 発達しつつある風波の場の相似構造に基づいてTOBA (1978) が発表した風波の単一パラメータ発達方程式によって，海洋波浪の予測を行なう具体的方法を開発した．この方法の現実の海洋に対する適用性を，スケールの異なる2つの海域，すなわち，紀伊水道アプローチと北大西洋における波浪の観測資料を事後予測することにより確認した．今回の方法は，波高 3～12 m の条件下において，1.3 m 以内の誤差で波浪を予測することができることがわかった．

* 東北大学理学部地球物理学教室
〒980 仙台市荒巻字青葉